environmental microbiology

Environmental Microbiology (2017) **19**(9), 3487–3499 doi:10.1111/1462-2920.13830

Toward establishing model organisms for marine protists: Successful transfection protocols for *Parabodo caudatus* (Kinetoplastida: Excavata)

Fatma Gomaa,[1,3†] Paulo A. Garcia,[2†] Jennifer Delaney,[3] Peter R. Girguis,[3] Cullen R. Buie[2] and Virginia P. Edgcomb[1*]

[1]*Department of Geology and Geophysics, Woods Hole Oceanographic Institution, Woods Hole, MA 02543, USA.*

[2]*Department of Mechanical Engineering, Massachusetts Institute of Technology, Cambridge, MA 02139, USA.*

[3]*Department of Organismic and Evolutionary Biology, Harvard University, Cambridge, MA 02138, USA.*

Summary

We developed protocols for, and demonstrated successful transfection of, the free-living kinetoplastid flagellate *Parabodo caudatus* with three plasmids carrying a fluorescence reporter gene (pEF-GFP with the EF1 alpha promoter, pUB-GFP with Ubiquitin C promoter, and pEYFP-Mitotrap with CMV promoter). We evaluated three electroporation approaches: (1) a square-wave electroporator designed for eukaryotes, (2) a novel microfluidic transfection system employing hydrodynamically-controlled electric field waveforms, and (3) a traditional exponential decay electroporator. We found the microfluidic device provides a simple and efficient platform to quickly test a wide range of electric field parameters to find the optimal set of conditions for electroporation of target species. It also allows for processing large sample volumes (>10 ml) within minutes, increasing throughput 100 times over cuvettes. Fluorescence signal from the reporter gene was detected a few hours after transfection and persisted for 3 days in cells transfected by pEF-GFP and pUB-GFP plasmids and for at least 5 days post-transfection for cells transfected with pEYFP-Mitotrap. Expression of the reporter genes (GFP and YFP) was also confirmed using reverse transcription-PCR (RT-PCR). This work opens the door for further efforts with this taxon and close relatives toward establishing model systems for genome editing.

Received 27 April, 2017; revised 12 June, 2017; accepted 13 June, 2017. *For correspondence. E-mail vedgcomb@whoi.edu; Tel. (+1)508 289 3734; Fax (+1)508 457 2183. †These authors contributed equally to this work, and share first authorship.

Introduction

Protists are unicellular eukaryotes that are ubiquitous in the marine realm, their molecular signatures have been described from all marine habitats investigated, and they are recognized as pivotal members of aquatic microbial communities in models of carbon cycling (Worden *et al.*, 2015). Phototrophic protists contribute to primary production, and heterotrophic protists shape organic matter pools and populations of their prokaryotic and eukaryotic prey, thus indirectly influencing activities at the foundation of microbially driven major nutrient cycles (Azam and Malfatti, 2007). Free-living protists exhibit complex interactions with other protists, Metazoa, Bacteria, Archaea, and viruses. Our understanding of the extent of marine protist diversity has expanded tremendously over recent decades, due in significant part to information from high-throughput sequencing approaches based on bulk extracted DNA/RNA. Protists also exhibit symbioses with prokaryotes and with other protists and Metazoa. Marine protist taxa with sequenced genomes reveal that microeukaryotes can have complex and large genomes that can be many times greater in size than even the human genome. The function of a significant portion of those genes remains unknown, and is referred to as "genetic dark matter" (Clark *et al.*, 2013).

To uncover the scientific principles that govern the interactions of protists with other microbes and that mediate nutrient flow in the sea, an understanding of the function of this genetic "dark matter" facilitated by genetically tractable model representatives is required. Their development will allow us to systematically decipher the gene–gene and gene–environment interactions, and to understand processes underlying the roles of certain protists in biogeochemical cycling and the evolution and ecology of the microbial Eukarya. Low efficiency transfection protocols exist for a few marine protists; *Ostreococcus tauri*,

Phaeodactylum tricornutum, *Amphidinium* sp. and *Symbiodinium microadriaticum* (Te *et al*., 1998; De Riso *et al*., 2009; van Ooijen *et al*., 2012). Transfection of two dinoflagellates has been successful using silicon carbide whiskers to deliver plasmid constructs (Te *et al*., 1998), and transfection of *Perkinsus marinus*, a marine protist parasite, has been achieved using electroporation (Fernandez-Robledo *et al*., 2008; Cold *et al*., 2016). Recent gene editing protocols have been established for few diatoms (Hopes *et al*., 2016; Liu *et al*., 2016), and progress toward useful forward genetics approaches for choanoflagellates have been established (Hoffmeyer and Burkhardt, 2016). Additional models are needed for more widely distributed, ecologically important free-living lineages. Methods of gene tagging and gene silencing using CRISPR/Cas9 have been developed for a few, mainly parasitic protists (*Trypanosoma cruzi*, *Leishmania* spp., *Plasmodium* spp., *Cryptosporidium parvum*, *Chlamydomonas reinhardtii*) (Lander *et al*., 2015; 2016a; 2016b; Peng *et al*., 2015), but again, there is a lack of methods for most protist taxa. Genetic manipulation of marine protists will make it possible to link genes of unknown function to cell behaviour (e.g., colony formation, morphogenesis, cell–cell interactions), physiology (e.g., life cycle and reproduction type), particular biogeochemical cycles, and processes of interest, such as, nitrogen and carbon cycling, and production of climate active trace gases or initiation of harmful algal blooms (Gong *et al*., 2017).

The first step in developing transgenic marine protists is the establishment of reliable and reproducible transfection protocols. Transfection can be accomplished using chemical-based methods (which include lipofection, calcium phosphate, etc.), electroporation, microinjection, biolistic, laserfection/optoinjection, and virus-based methods (Kim and Eberwine, 2010). Electroporation using pulsed electric fields is a technology that has become a powerful and mature tool used for genetic engineering of prokaryotes and eukaryotes. Via electroporation, electrical pulses of a specified voltage and duration transiently disrupt the membrane of cells and deliver foreign DNA (i.e., plasmids) into the cells within milliseconds. With the advent of electroporation, bacterial strains could be transformed with plasmids carrying marker genes (Teissie and Tsong, 1981; Neumann *et al*., 1982; Josenhans *et al*., 1998) and methods have evolved since then to include a wide range of tools including most recently, RNAi and CRISPR/Cas9 (Peng *et al*., 2015; Liang *et al*., 2017). Such approaches can allow researchers to gain an understanding of the role of a gene of interest in the physiology or behaviour of an organism, and in turn, the role the gene plays in the organism's ecology.

While electroporation methods for some bacteria, such as *Escherichia coli*, are technically simple and thus commonplace, the efficacy of electroporation, broadly speaking, depends on many variables. The critical parameters in electroporation are the electric field magnitude and pulse characteristics such as the shape, duration, and number of pulses (Weaver *et al*., 2012). Traditionally, electroporation is performed in plastic cuvettes outfitted with parallel plate metal electrodes. The separation distance between the plate electrodes is fixed at 1 mm, 2 mm, or 4 mm and the DNA-cell suspension is placed between the electrodes. Upon application of a voltage, an electric field is generated between the plates at a magnitude equal to the voltage-to-distance ratio (Corovic *et al*., 2007). Other experimental parameters affecting the outcome include the DNA concentration and the electrical conductivity (salt concentration) of the medium surrounding the cells (i.e., electroporation buffer). Buffers with lower ionic concentrations reduce the arcing potential (electrical breakdown that occur due to high or excess salt concentration), reduce deleterious heating, and generally increase the transfection efficiency (Kotnik *et al*., 2015). Notably, eukaryotic cells (including many protists) are highly sensitive to the experimental conditions that are optimal for electroporation, such as lower ionic concentrations. The low efficiency of electroporation resulting from the myriad of technical challenges has hindered progress in developing electroporation-based methods appropriate for aquatic protists.

Accordingly, we aimed to develop an efficient method for electroporation of marine protists. For this effort, we selected *Parabodo caudatus*, a free-living biflagellate kinetoplastid (Parabodonida, Kinetoplastea, Euglenozoa), and free-living close relative of parasitic trypanosomatid flagellates. *P. caudatus* feeds on bacteria (e.g., *Klebsiella pneumoniae*, *E. coli*, *Enterobacter aerogenes*, and others). *P. caudatus* cells divide by longitudinal binary fission. Members of this family have fast growth rates and are easy to culture and maintain in laboratory. They prey on bacterial cells and are ubiquitous in many environments including fresh and marine water columns and sediments, seawater from deep-sea hydrothermal vents, and as contaminants in food (von der Heyden *et al*., 2004; Tikhonenkov *et al*., 2016). The genome of a congener of *P. caudatus*, *Bodo saltans*, revealed that 60% of all coding genes had homologs in trypanosomatids, evolutionary close relatives to kinetoplastids (Jackson *et al*., 2008; 2016; Opperdoes *et al*., 2016). The remainder of genes was found to be homologs of genes in other eukaryotes (i.e., fungi, animals, and plants) but not trypanosomatids, or *Bodo*-specific genes with no matches to sequences in public databases. These *Bodo*-specific genes were predicted as hypothetical proteins expressed on the cell surface (Jackson *et al*., 2008; 2016; Opperdoes *et al*., 2016). These findings suggest that *Parabodo* and other free-living bodonids represent appealing model organisms for exploring potential roles of those unidentified genes.

To determine the efficacy of electroporation as a means of transforming marine protists, we tested three different transfection technologies. First, we evaluated a commercially available square-wave technology that has been successfully used to increase transfection rates by 2–3 times in living cells ranging from very fragile mammalian stem cells (Kaneko *et al*., 2014) to intact vertebrate embryos (when compared with traditional exponential decay electroporation) (Sanders *et al*., 2013). Very few studies to date, however, have examined electroporation responses of free-living microeukaryotes, which are markedly different than mammalian cell lines in their robustness and their transfection amenability (Miyahara *et al*., 2013). While the exponential decay electroporation methods enable voltage, resistance, and capacitance to be independently selected, the square-wave generator enables additional parameters such as pulse duration, pulse number, and pulse polarity. The square-wave system may be used to apply two types of multi-pulse electroporation protocols (Fig. 1B). The first sequence uses poring pulses, which are multiple high-voltage, short duration (5 ms) pulses responsible for formation of the initial pores (membrane defects) in the cell membrane. The second sequence uses transfer pulses, which are multiple low-voltage, long duration (50 ms) pulses that deliver the target molecules into cells with minimal damage. The low-voltage pulses are similar to those used in electrophoresis, which facilitates the movement of charged molecules such as DNA into the cells.

The second method that we evaluated utilizes a novel microfluidic platform for identifying critical electroporation conditions for successful transformation, recently developed by a subset of the authors (Garcia *et al*., 2016). We further developed our microfluidic platform to conduct continuous flow transformation of microorganisms (Garcia *et al*., 2017). This technology uses microfluidic channels with geometric constrictions (see *Experimental procedures* section for physical dimensions) to amplify the electric field to achieve electroporation (Fig. 1A). In our bilaterally converging microfluidic system, a single applied voltage results in a linear electric field gradient along the length of the microchannel constriction and results in a maximum $\sim 6\times$ amplification of the applied voltage (1 V = 6 V/cm). Thus, depending on the applied voltage and the location within the constriction, the strength of the electric field will be able to induce cell electroporation. Square wave pulses are delivered from electrodes with alternating polarity between the pulses to reduce electrolytic effects at the electrode-buffer interface (Supporting Information Fig. S1). For example, square wave pulses with 5 ms ON and 5 ms OFF cycles are applied to the microchannel through the dispensing needles, which results in 50% of the cells experiencing the electric field during their transit through the channel. Increasing the duty cycle would result in a larger fraction of the cells being exposed to the electric field, and also more sample heating. To mitigate potential deleterious heating, the flow rate must be selected carefully to remove the heated sample from the constriction without compromising cell viability. The microfluidic device conveniently provides a simple platform to efficiently test transfection conditions and optimize parameters for genetic manipulation of recalcitrant organisms such as many protists.

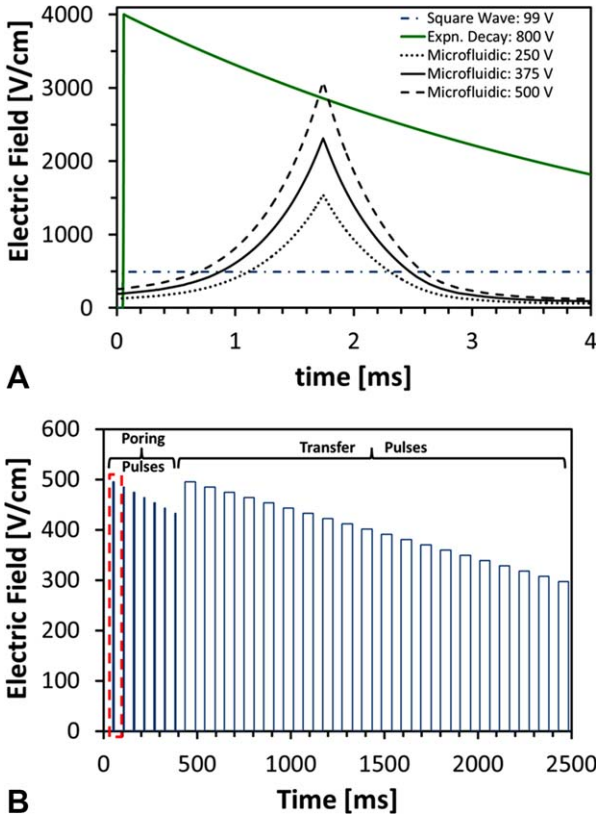

Fig. 1. Electric field waveforms employed for transient and stable transfection of *P. caudatus*.
A. Three independent electroporation systems were used for reproducible transfection, including our microfluidic electroporation platform (Garcia *et al*., 2017), the NEPA21 square-wave transfection system (Bulldog Bio), and the MicroPulser™ exponential decay electroporator (Bio-Rad).
B. The signature waveforms for the NEPA21 square wave transfection system include both "poring" and "transfer" pulses for electroporation. Note: The time scale in Fig. 1A is a zoomed-in version of the red-dashed box from Fig. 1B.

The third system we investigated was a MicroPulser Bio-Rad (CN 165–2100) exponential decay system (Fig. 1). Among electroporation technologies, exponential decay technologies have been routinely used in laboratories the longest. Here we report successful transient transfection of the free-living kinetoplastid flagellate *P. caudatus* with three plasmids carrying fluorescent protein (FP) reporter genes, using three electroporation approaches: (1) a new microfluidic transfection system using hydrodynamically-

controlled waveforms, (2) a square-wave transfection system, and (3) traditional exponential decay electroporation. This study is the first experimental comparison of successful transient transfection of marine microeukaryotes employing three different electroporation methods. It lays the groundwork for future efforts aimed at stable transfection with a variety of gene targets, and genetic manipulation of this taxon and its close relatives.

Results

Cell viability after cytomix buffer incubation

Tolerance of *P. caudatus* to different electroporation buffers was tested. *P. caudatus* cells were viable after incubation in 50% and 10% cytomix (Knight and Scrutton, 1986) buffer concentrations for at least 15 min. However, *P. caudatus* incubated in 100% cytomix were viable for about 10 min, after which increasing cell mortality was observed. Therefore, all our subsequent experiments were performed in 50% cytomix buffer, 10% or 1% seawater, or MilliQ water to maintain high cell viability.

Electroporation buffer conductivity

The exponential decay (MicroPulser Bio-Rad CN 165–2100) system resulted in arcing at the highest voltage tested (1000 V), because all cytomix buffer concentrations tested had relatively high electrical conductivity. However, when the voltage was reduced (800 V, 500 V, and 300 V) arcing was eliminated and the resulting pulses lasted between 0.7 ms and 1.2 ms. Buffers composed of 10% seawater and 1% seawater both resulted in pulse durations between 0.7 ms and 3.5 ms at all applied voltages between 1000 V and 300 V. These pulse durations are all shorter than the typical 5.0 ms that results when using low conductivity buffer, such as MilliQ water at all voltages tested.

For the square wave electroporation system (NEPA21 transfection system, Bulldog Bio), cytomix buffers at high or low concentrations and the 10% seawater were too conductive, resulting in arcing at 150 V and 300 V during a continuous 5.0 ms square pulse (Miyahara *et al.*, 2013). In contrast, when voltage strength of both poring and transfer pulses was reduced to 99 V, with multiple 5.0 ms square pulses, the treatment was successful in the 100% cytomix, 50% cytomix, 10% cytomix, and 10% seawater buffers (Table 2). Buffers with low conductivity, such as, 1% seawater and MilliQ water were also able to complete the entire treatment without arcing at any of the tested voltages (99 V, 150 V, and 300 V).

Post-electroporation cell viability quantification

Using the exponential decay system, *P. caudatus* cells did not survive exposure to 1000 V in any of the above mentioned electroporation buffers (Supporting Information Table S1). In contrast, 40–50% of cells were viable post-electroporation when a single exponentially decaying pulse was applied at 800 V ($E = 4000$ V/cm) in all tested electroporation buffers. When the maximum voltage was limited to 500 V ($E = 2500$ V/cm) cell viability increased to between 60% and 70%. Applied voltages of 300 V ($E = 1500$ V/cm) resulted in the highest cell viability of about 80–90%.

Using the square-wave system, we initially tested the same parameters that were successfully applied for transformation of diatoms (Miyahara *et al.*, 2013). Electroporated cells exposed to 150 V ($E = 750$ V/cm) or 300 V ($E = 1500$ V/cm) in MilliQ water or 1% seawater survived. However, these electric fields failed to successfully transform *P. caudatus* with plasmid DNA, potentially because the transfer pulses used very low voltage (8 V). We therefore tested several other poring and transfer pulse voltage combinations, pulse numbers, and durations. Cells of *P. caudatus* electroporated with a maximum applied voltage of 99 V for poring and transfer pulses ($E = 500$ V/cm) in any of the investigated electroporation buffers (cytomix, seawater, and MilliQ water) were viable with no observed cell damage or loss. These parameters were also successful for establishing plasmid DNA transfection for *P. caudatus*.

We did not specifically assess cell viability after applying the microfluidic platform since cells are exposed to different electric fields with a single applied voltage (Garcia *et al.*, 2016). In addition, depending on the duty cycle selected, some of the cells flowed through the device without being exposed to any electric field. Therefore, we tested electric field parameters that resulted in high cell viability using the exponential decay platform in subsequent experiments in the microfluidic device.

Real-time permeabilization confirmation with SYTOX® post-electroporation

We aimed to establish the first transfection protocols for marine protists using the microfluidic system, and to identify the critical electric field that is required for the onset of electroporation. Initially, the ability to permeabilize *P. caudatus* cells was tested using the intercalating dye SYTOX® blue nucleic acid stain, which fluoresces upon binding to intracellular DNA. We delivered a single pulse with applied voltages of 500 V ($E_{max} = 3000$ V/cm) and 1000 V ($E_{max} = 6000$ V/cm) in the absence of flow to expose cells to a range of electric fields. The fluorescence images depicted in Fig. 2E and 2F confirm the ability to electroporate the cells at electric fields ranging from 1000 V/cm to 6000 V/cm with a pulse duration of about 5 ms. The extremely high permeabilization efficiency at the ideal electric field can be seen in Fig. 2F, in which the majority of cells in the microfluidic channel have been successfully

Table 1. Experimental conditions that resulted in successful transient *P. caudatus* transfection in the exponential decay and microfluidic systems with a single pulse.

System	Voltage (V)	E_{max} (V/cm)	Pulse length (ms)	Buffer	Plasmid	Duty cycle %	Transfection efficiency %*
Microfluidic electroporation	313	1000	20	Cytomix	pEF-GFP	95	20–30
	250	1500	2	H_2O	Mitrotrap	95	30–40
	375	2250	2	H_2O	Mitrotrap	95	40–50
	375	2250	2	H_2O	pUB-GFP*	50	20–30
	375	2250	4	H_2O	pUB-GFP*	50	20–30
Exponential decay	800	4000	2 or 3	H_20	pEF-GFP	n/a	5–10
	800	4000	2 or 3	H_20	Mitrotrap	n/a	5–10

*Note transformation efficiency for microfluidic electroporation with pUB-GFP is underestimated because only 50% of cells were exposed (50% duty cycle) to the electric field along the gradient that resulted in successful transfection. Transfection with the pEF-GFP and pEYFP-Mitotrap utilized a 95% duty cycle.

permeabilized (Supporting Information Video S1). However, because the dead cells are also labelled with SYTOX®, this electroporation assay does not inform on the upper limit of the electric field within the range where cells are labelled and still viable. Transfection with plasmid DNA using the microfluidic technology provided more conclusive evidence of transfection success.

Transformation of P. caudatus *with plasmids*

Circular DNA plasmids pEF-GFP, pUB-GFP, and pEYFP-Mitotrap were introduced separately into *P. caudatus* using the three different electroporation systems with parameters presented in Tables 1 and 2. All of our plasmids were expressed in the cytoplasm of *P. caudatus* cells, after they were transcribed in the host's nucleus. In all cases of successful transfection, transformants were viable and their growth rate was similar to that of wild-type cells. No morphological differences in the cell shape were detected between the transfected and wild type cells (Figs 3 and 4). Expression of the GFP gene, driven by either the EF1 alpha promoter or the ubiquitin C promoter, and the YFP gene, driven by the CMV promoter, was documented using a fluorescence microscope 12 h post-electroporation (Figs 3 and 4). Expressed GFP signal levels decreased gradually over the 48 h post-electroporation, but YFP expression was maintained for 5 days (the longest time that expression was monitored). Microscopy revealed that GFP expression driven by the ubiquitin C promoter was stronger than the GFP expression pattern driven by the EF1 alpha promoter. Reverse transcription-PCR performed using RNA isolated from *P. caudatus* cells transfected using the microfluidic system and the pUB-GFP plasmid revealed the presence of GFP transcripts 3 days post-transfection (Fig. 5). These results clearly indicate that the pUB-GFP plasmid was delivered into *P. caudatus* nucleus by electroporation and was transcribed to GFP mRNA *in vivo*.

The fluorescence signal resulting from transfection of *P. caudatus* with the pEYFP-Mitotrap plasmid was stable for 5 days post-transfection. Transcription of the YFP gene was confirmed by RT-PCR using RNA isolated 5 days post-transfection (Fig. 5). Stability was not monitored past 5 days in this study. Given optimization of antibiotic selection markers was outside the scope of this short-term project, post-transfection cultures were maintained in the absence of a selection marker, and hence were not suitable for long-term observation or experiments to confirm stable transfection.

The microfluidic technique was implemented in the transformation of *P. caudatus*, but unlike the square-wave and exponential decay systems, this system does not employ a uniform electric field. As cells flow through the microfluidic device, they are exposed to multiple electric fields, making it challenging to assess viability as a function of a specific, uniform electric field. Based on our electroporation assays, initial unsuccessful attempts were made using maximum electric fields of 6000 V/cm or 9000 V/cm at the constriction with a 20% duty cycle (Supporting Information Table S2). To improve the probability of transfection, the duty cycle was increased to 50% with maximum electric fields of 750 V/cm, 1500 V/cm, or 2250 V/cm. These experiments conducted with a 50% duty cycle resulted in transfection efficiencies ranging between 20% and 30%. Finally, we increased the duty cycle to 95% to increase the fraction of treated cells with maximum electric fields ranging between 500 V/cm and 3000 V/cm.

Table 2. Experimental conditions that successfully resulted in transient *P. caudatus* transfection with EF-1alpha plasmids in the square wave transfection system.

Voltage (V)	E_{max} (V/cm)	Pulse number	Pulse length (ms)	Decay rate (%)	Buffer	Pulse type	Transfection efficiency
99	500	7	5	10	Cytomix	Poring	40%
99	500	20	50	40	Cytomix	Transfer	

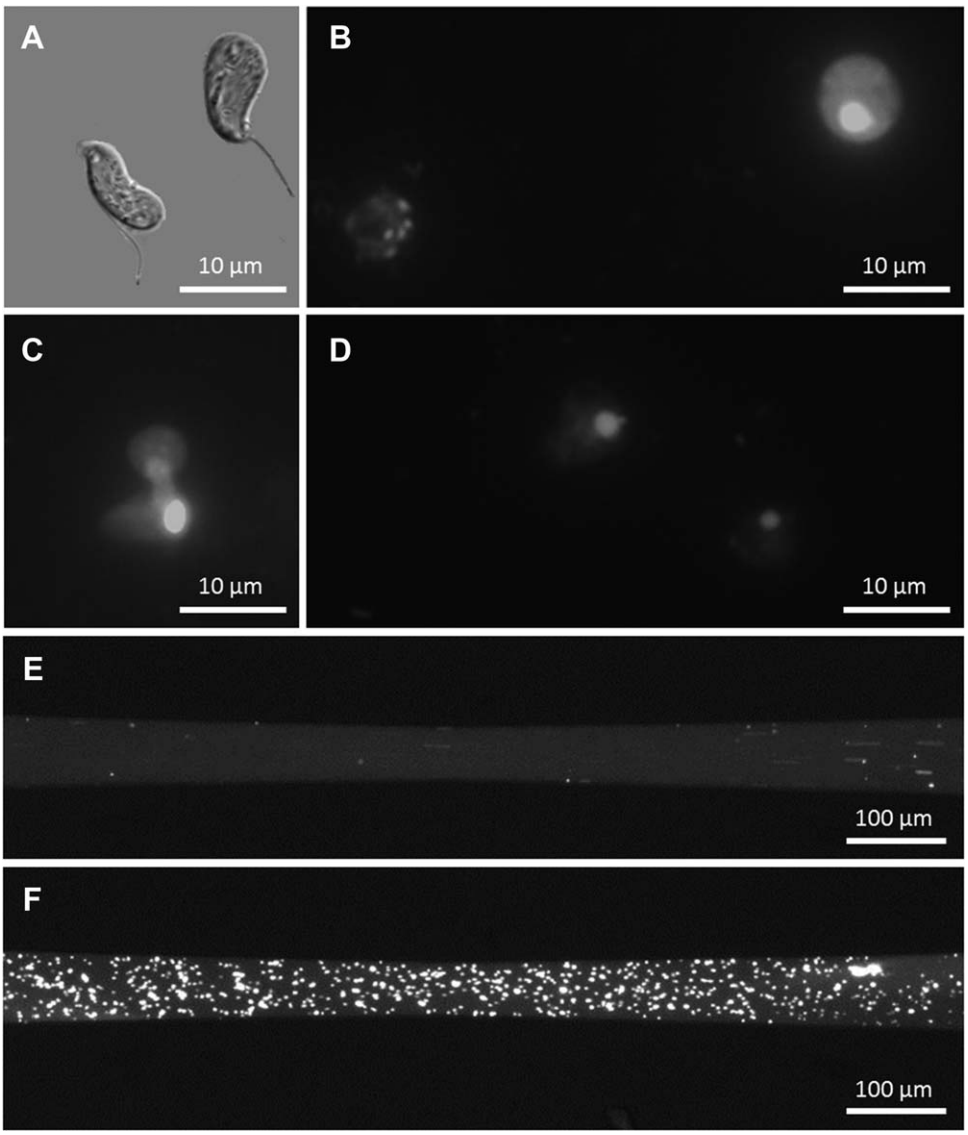

Fig. 2. Permeabilization confirmation of *P. caudatus* cells with SYTOX® Blue. A. Phase contrast and (B–D) fluorescence images of *P. caudatus* electroporated with 5 µM SYTOX® Blue nucleic acid stain at 300 V (E_{max} = 1500 V/cm), 500 V (E_{max} = 2500 V/cm), and 800 V (E_{max} = 4000 V/cm), respectively, using the exponential decay electroporation system in 2-mm cuvettes. Fluorescence images (E) before and (F) after electroporation in the microfluidic system using a single 5 ms exponential decay pulse at 500 V (E_{max} = 3000 V/cm).

Transfection efficiencies ranging between 30% and 50% were also achieved with maximum electric fields of 1500 V/cm and 2250 V/cm using 5 ms pulses in MilliQ water. In addition, we achieved transfection efficiencies ranging between 20% and 30% using a maximum electric field of 1000 V/cm with 20 ms pulses in 50% cytomix buffer in a straight channel.

Transformation efficiencies (percentage of successfully transformed cells) were comparable for the microfluidic platform and the commercially available square-wave technology. The microfluidic platform was the most efficient method with 30–50% of the cells successfully transformed (Table 1). The square-wave platform resulted in transformation efficiency of $\geq$40% (Table 2). Finally, the exponential decay electroporation resulted in $\leq$5% transformation efficiency making it the least optimal transfection platform evaluated (Table 1).

Discussion

In this study, we achieved successful transfection of *P. caudatus* using three electroporation systems; our microfluidic platform, a square-wave system, and traditional exponential decay methods. The process of developing transient transfection protocols in *P. caudatus* involved initial testing and determination of proper electroporation buffers and parameters (voltage strength, pulse duration, and number). Our results suggest that the type of electroporation buffer is critical for maintaining high cell viability throughout the experiment and is essential for determining the optimum electric field range. We have demonstrated that successful electroporation conditions were different for the three electroporation systems utilized, and are largely dependent on the electric field strength, as well as the pulse number and pulse duration. Transient transfection was carried out using three

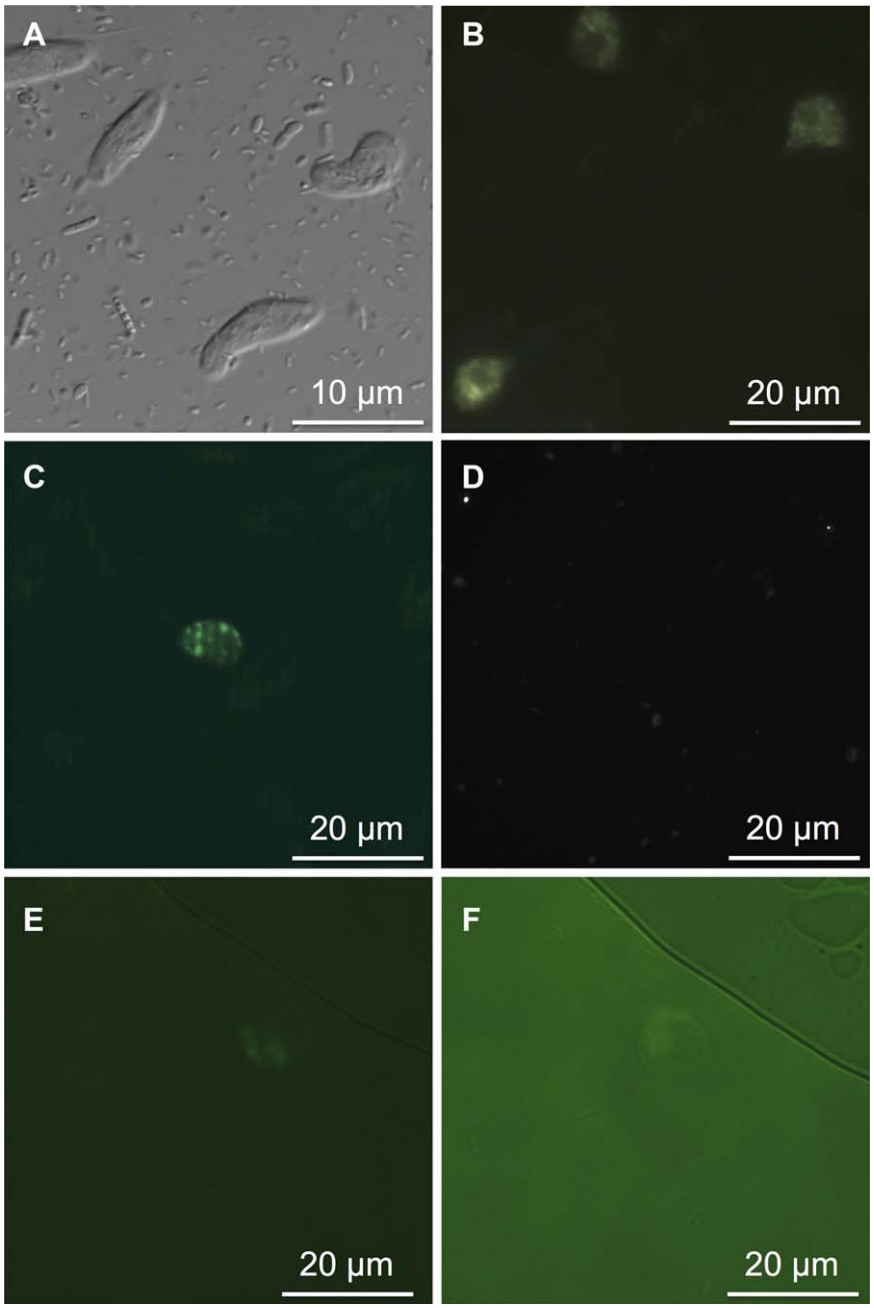

Fig. 3. Microfluidic transfection of *P. caudatus*.
A. *P. caudatus* (brightfield), (B) transient pEYFP-Mitotrap transfection at 250 V (E_{max} = 1500 V/cm), (C) transient pUB-GFP transfection using 375 V (E_{max} = 2250 V/cm), (D) autofluorescence control for *P. caudatus*, (E) transient transfection using pEF-GFP and 313 V (E_{max} = 1000 V/cm) in the straight channel, and (F) merged image of brightfield and fluorescence image from (E) for visualizing cell morphology. [Colour figure can be viewed at wileyonlinelibrary.com]

plasmids, pUB-GFP, pEF-GFP, and pEYFP-Mitotrap, which utilize promoters that are recognizable to most eukaryotes, to determine and optimize electroporation parameters. We now know that all three promoters, CMV, ubiquitin C, and EF1 alpha, work successfully with *P. caudatus*. Our transient transfection experiments demonstrated the feasibility of introduction and expression of foreign DNA into *P. caudatus* using each of the three systems (microfluidic, square wave, and the exponential decay), and the optimal electroporation parameters to apply for future stable transfection of *P. caudatus*.

Although the pEYFP-Mitotrap plasmid includes neomycin resistance as a selection marker gene and Tom70p as a target gene for the mitochondrial outer membrane (Robinson *et al.*, 2010), the long-term transfection stability and the efficacy of transfection selection based on antibiotic resistance were not examined in our study. Assessing longer-term transfection stability using selective marker genes requires initial screening with various antibiotics to determine the most effective antibiotic and concentration, and this was outside the scope of this project. Furthermore, to confirm stable transfection, one should investigate integration of the plasmid genes into the host

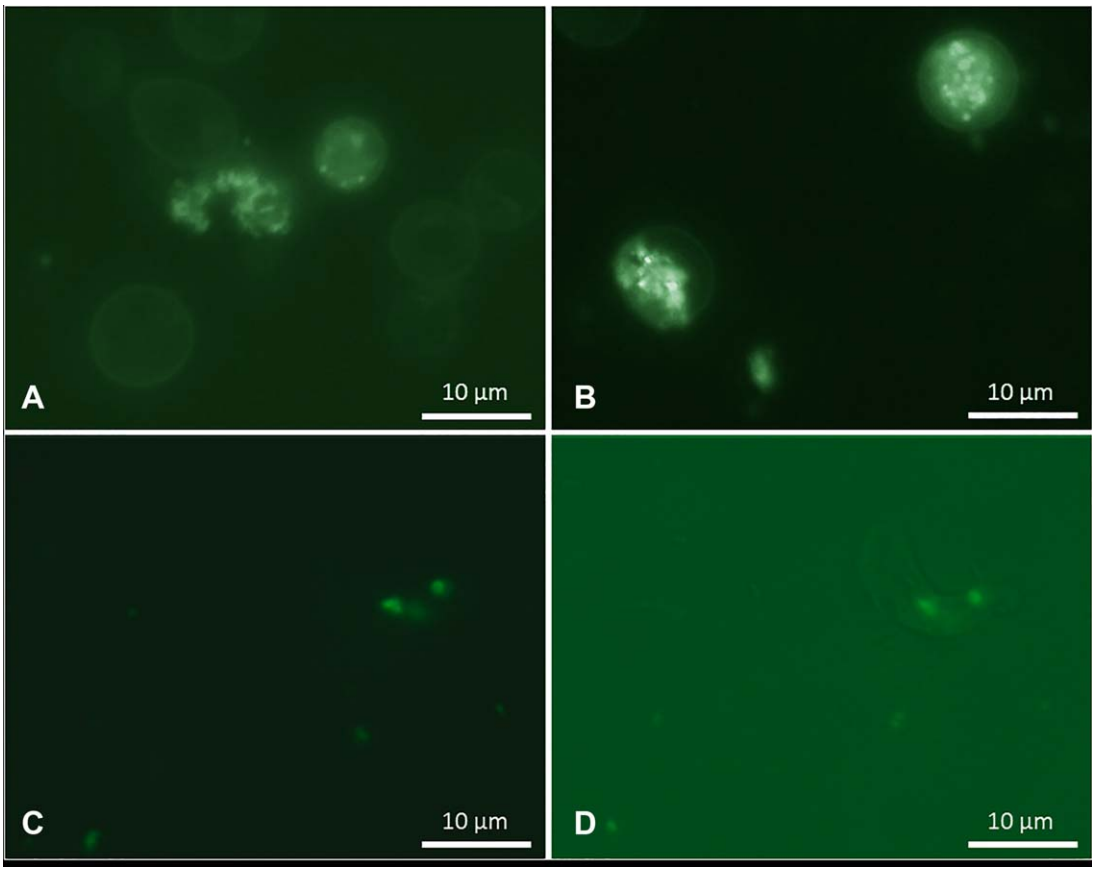

Fig. 4. Exponential decay and square wave transfection of *P. caudatus*. Fluorescence imaging confirmation of *P. caudatus* after (A) transient transfection with pEF-GFP using the MicroPulser^{TM} exponential decay electroporator, after (B) transient transfection with pEYFP-Mitotrap using 800 V (E_{max} = 4000 V/cm) in the exponential decay electroporator, and after (C) transient transfection with pUB-GFP using the NEPA21 square-wave transfection system at 99 V (E_{max} = 500 V/cm). Panel (D) shows merged fluorescence image from (C) with the brightfield image.

genome by Southern blot or PCR and sequencing methods. Given that expression of the YFP gene was detected 5 days post-transfection via RT-PCR (Fig. 5), which represents stability over at least 5–6 generations, it is possible that this plasmid integrated into the nuclear genome, but this would need to be confirmed with Southern blotting. Similarly, we established successful transfection of the choanoflagellate *Monosiga brevicollis* using the microfluidic system with the same plasmid, pEYFP-Mitotrap, which was expressed for at least 4 days post-transfection (data not shown). This was supported by RT-PCR but not microscopically, due to overlap between the strong cell autofluorescence signal and the reporter gene signal.

The square-wave system

The square wave system with the specific electric field conditions given in Table 2 successfully delivered pUB-GFP plasmid DNA into the *P. caudatus* cytoplasm and achieved transient GFP expression with a transfection efficiency of about 40% (Fig. 4C and D). In these conditions, both poring and transfer pulses had an equal electric voltage strength of 99 V (E = 500 V/cm). In contrast, attempts to establish transgenic *P. caudatus* using the previously applied electroporation parameters for diatom transformation (Miyahara *et al.*, 2013) with high poring pulses voltage (150 V or 300 V) and low transfer pulses voltage (8 V) were unsuccessful. These results suggested that even though *P. caudatus* and the diatom *Phaeodactylum tricornutum* are single-celled marine eukaryotes, they possess different cell characteristics and therefore a different electric field strength and pulse number are required for successful intracellular delivery of exogenous DNA.

The exponential decay system

The exponential decay electroporation system was also used successfully to establish transgenic *P. caudatus* using two plasmids: the pEF-GFP and the pEYFP-Mitotrap (Fig. 3A and B). Comparison of results for the square wave and the exponential decay systems shows the exponential decay system results in a lower transformation efficiency of 5%, and that the survival rate of the electroporated cells after exponential decay pulses at 800 V (E = 4000 V/cm)

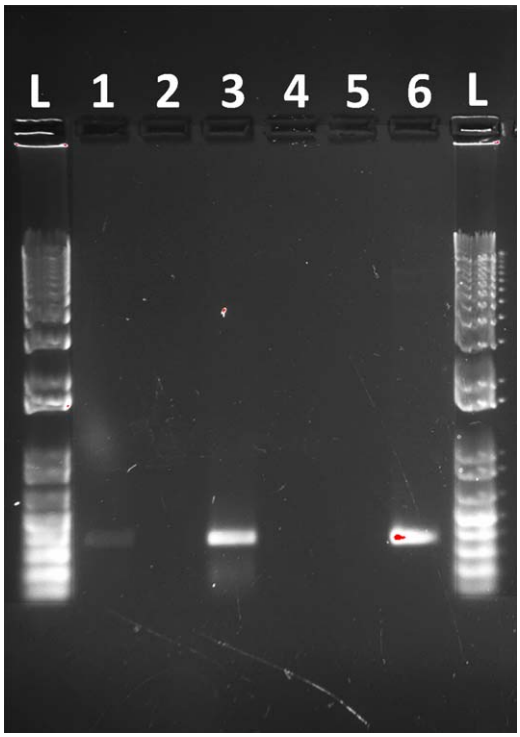

Fig. 5. Gel electrophoresis image showing the RT-PCR results detecting reporter genes expression in *P. caudatus* transformants. (L) 1kb ladder (Invitrogen, cat. #10787018); (1) GFP expression profile in *P. caudatus* cells transformed with pUB-GFP plasmid at 375 V using the microfluidic electroporation system; (2) Control reaction was performed without addition of RT to verify the absence of DNA in the RNA preparations in *P. caudatus* cells transformed with pUB-GFP transient plasmid using 375 V with the microfluidic electroporation system; (3) pEYFP expression profile in *P. caudatus* cells transformed with pEYFP-Mitotrap plasmid at 250 V with the microfluidic electroporation system; (4) Control reaction was performed without addition of RT to verify the absence of DNA in the RNA preparations in *P. caudatus* cells transformed with pEYFP-Mitotrap plasmid at 250 V with the microfluidic electroporation system; (5) PCR negative control; (6) PCR positive control using the GFP plasmid DNA. The PCR products were separated on a 1% agarose gel, visualized under UV light, and DNA fragments of both reporter genes were at the expected size of 367-bp. [Colour figure can be viewed at wileyonlinelibrary.com]

is less than 50% (based on light microscopy observation of swimming cells). Relative to the square wave system, these results clearly indicate the increased effectiveness of the lower voltages and multiple pulses produced by the square wave electroporation system for delivering the extracellular DNA to larger numbers of cells with minimum cell damage.

The microfluidic electroporation system

The microfluidic electroporation system resulted in the highest transfection efficiencies ranging from 20% to 50%. The applied electric fields were much smaller than the ones employed during the SYTOX® assay to increase cell viability. We demonstrated successful *P. caudatus* transfection employing electric fields of 1500 V/cm, resulting in transformation efficiencies of 30–40%, and 2250 V/cm, resulting in transformation efficiencies of 40–50% efficiency using 5 ms pulse durations in MilliQ water and the bilaterally constricting channel geometry. In addition, by decreasing the electric field to 1000 V/cm and by employing longer 20 ms pulses, we achieved 20–30% transfection efficiencies in 50% cytomix buffer using the straight channel constriction. These results demonstrate that different geometric constrictions can be used successfully to modulate the electric field that the cell is exposed to for successful transfection.

The major advantage of the microfluidic platform is that it allows continuous flow-through transfection in comparison to traditional, commercially available cuvette-based technologies, while achieving comparable or better transfection efficiencies. In addition, since the flow-through transfection process is continuous in nature, there is flexibility in the sample volume. This has exciting implications for processing large sample volumes ($>$10 ml) within minutes, increasing throughput by 100 times in comparison to cuvettes (Garcia *et al.*, 2017). This has advantages for future genome editing applications including library generation, and the ability to transfect cells directly from aqueous environments.

Conclusions

Development of successful transfection protocols for marine protists will enable advances in our understanding of their ecology. Here, we successfully transfected *P. caudatus* for the first time using three different electroporation-based transfection methods and three different DNA plasmids pEF-GFP, pUB-GFP, and pEYFP-Mitotrap. Between the two traditional cuvette-based technologies (exponential decay and square wave), multi-pulse square wave electroporation resulted in higher transformation efficiency and cell viability. The microfluidic electroporation system produced the highest transfection efficiency (20–50%) when the optimal combination of buffer, electric field, and flow rate (among those tested in this study) was employed. This implies that microfluidic transfection holds great promise for efficiently optimizing and conducting electroporation of a potentially wide range of microbial eukaryotes. The microfluidic system is economical and can be installed and easily used by researchers and academics. The device features hydrodynamically-controlled electric fields that allow cells to experience a time-dependent pulse waveform that is otherwise difficult to achieve using standard electronics. The ability to efficiently test a wide range of electroporation parameters, or to quickly transfect a target (or a collection of targets) with a range of genetic elements has significant advantages over cuvette-based methods for the field of genome editing. High-throughput transfection technologies such as our

microfluidics system offer the possibility of parallel processing of multiple samples (cultures or environmental samples), making possible effective investigations into the ecological roles of protists.

Experimental procedures

P. caudatus strain and growth media

Parabodo caudatus culture (ATCC 50361) was used in this study. This ATCC strain was isolated from a freshwater sediment location, but *Parabodo* is described from marine habitats (Kopylov *et al.*, 1980). Initially, *P. caudatus* was grown in 50% ATCC seawater 802 media. Subsequently, seawater was replaced with distilled water to reduce the high electrical conductivity during the electroporation. Briefly, this is a cerophyl-based media enriched with 3.5 mM sodium phosphate dibasic (Na_2HPO_4) and with *K. pneumoniae* (ATCC-BAA 1706) added as a food source. *K. pneumoniae* is a gram negative, rod-shaped facultative anaerobe bacterium commonly found in animals and the environment, and routinely used as bacterial prey. Cultures were incubated at 22°C and sub-cultured weekly in fresh T-25 vented tissue culture flasks (Falcon brand, Fisher Scientific) containing 30 ml of fresh media.

Cell viability assay after cytomix buffer incubation

Cell viability of *P. caudatus* in cytomix buffers needed to be tested since they can be cultured in either MilliQ water or $\leq$50% seawater. Three replicates of *P. caudatus* cultures each 25 ml (i.e., biological replicates of *P. caudatus*, defined as different starting culture bottles, although it is noted that all originated from the same starting strain) in logarithmic growth phase (1×10^7 cells to 1.3×10^7) were harvested by centrifugation at 5000$\times g$ for 30 s and re-suspended in 200 μl of 100% cytomix, 50% cytomix, or 10% cytomix. To evaluate survival in these buffers, aliquots of 20–30 μl of the cell-buffer mixture were placed on a haemocytometer every 5 min for 15 min and were imaged under bright field microscopy (Nikon) using a 20× objective. Survival was determined by counting the total number of swimming cells in the haemocytometer and determining the fraction of live cells.

Electroporation buffer conductivity

A buffer with low electrical conductivity is recommended to minimize Joule heating during electroporation. We evaluated the electrical conductivity for the following buffers: 100% cytomix (120 mM KCl; 0.15 mM $CaCl_2$; 10 mM KH_2PO_4; 25 mM HEPES; 2 mM EGTA; 5 mM $MgCl_2$; pH adjusted to 7.6 with KOH), 50% cytomix (in MilliQ water), 10% cytomix (in MilliQ water), 10% seawater, 1% seawater, or 100% MilliQ water, at four different voltages (300 V, 500 V, 800 V, and 1000 V). Since the exponential decay system uses 2-mm gap cuvettes, the electric fields result in 1500 V/cm, 2500 V/cm, 4000 V/cm, and 5000 V/cm, respectively, after computing the voltage-to-distance ratio. Electric field amplitude and pulse duration were measured for each electroporation event with parameters given in Supporting Information Table S1. For square wave we followed a published protocol for diatom transformation by Miyahara *et al.* (2013), which uses 2-mm cuvettes with applied voltages of 150 V and 300 V. In the microfluidic device we only tested combinations of *P. caudatus* cells in the presence of SYTOX® or DNA as outlined below.

Electroporation parameters tested and post-electroporation cell viability quantification

Prior to electroporation of *P. caudatus* cells in the MicroPulser Bio-Rad (CN 165–2100) exponential decay system (Fig. 1), cell pellets from 25 ml of replicate cultures were re-suspended in 200 μl MilliQ water, 1% seawater, 10% seawater, 10% cytomix, or 50% cytomix and transferred to 2-mm gap cuvettes. The cells were electroporated with applied voltages of 300 V ($E = 1500$ V/cm), 500 V ($E = 2500$ V/cm), and 800 V ($E = 4000$ V/cm). The pulse duration in milliseconds (ms) after each electroporation was recorded (Supporting Information Table S1). The cells were immediately transferred to a 1.5 ml Eppendorf tube containing 1 ml of fresh growth media (ATCC 802 medium prepared with distilled water) for recovery. To determine cell viability, aliquots (20–30 μl) of electroporated cells were quantified using microscopy for each electric field applied.

The NEPA21 transfection system (Bulldog Bio), which utilizes square wave pulses, was used for electroporation of *P. caudatus* in 2-mm gap cuvettes with identical buffers as used for the exponential decay experiments. We initially used the same electroporation parameters that were successfully applied previously for transformation of diatoms (Miyahara *et al.*, 2013). However, these high applied voltages of 300 V or 150 V were found to compromise *P. caudatus* cell viability so modifications were necessary with a lower applied voltage (Table 2). It is important to note that transformation in *P. caudatus* was most successful when we employed "poring" ($t = 5$ ms) and "transfer" ($t = 50$ ms) pulses of the same amplitude (99 V) but with different pulse durations.

We recently developed a continuous flow system to transform microorganisms in high throughput in a microfluidic device (Garcia *et al.*, 2017). This system employs microfluidic channels that contain a bilateral constriction between the inlet and outlet electrode connections where the cell-DNA solution is driven by a syringe pump ($l = 3.0$ mm, $w_{min} = 50$ μm, $w_{max} = 2.0$ mm, and $h = 100$ μm). The constriction amplifies the electric field under an applied voltage between the inlet and outlet electrodes to levels sufficiently high to induce electroporation. As opposed to the previous two systems that deliver uniform electric fields in static cuvettes, this system drives cells through the constriction, which is the region of highest electric field. During *P. caudatus* transfection, the cells were driven through the microfluidic device at flow rates of 50 μl/min and 500 μl/min, which correspond to residence times (i.e., pulse durations) of 20 ms and 2 ms, respectively. Square wave pulses with, for example, 5 ms ON and 5 ms OFF cycles (50% duty cycle) are applied to the microchannel through the dispensing needle. Therefore, the cell viability cannot be accurately evaluated since only 50% of the cells experience the electric field. The pulses are delivered from electrodes with alternating polarity between the pulses to reduce electrolytic effects at the electrode-buffer interface (Fig. 1 and Supporting Information Fig. S1). After flowing through the microchannel (see Supporting Information Video S2), each 200 μl cell sample

is added to a 1.5 ml Eppendorf tube containing 1 ml of fresh growth media for cell recovery. The applied voltages evaluated had amplitudes of 250 V ($E_{max} = 1500$ V/cm), 375 V ($E_{max} = 2250$ V/cm), and 500 V ($E_{max} = 3000$ V/cm) for each polarity. The non-uniform constriction in the microfluidic devices generates a variable electric field that is capable of transfecting cells while minimizing exposure to the highest electric field.

Electroporation protocol optimization with SYTOX® Blue

We used the SYTOX® Blue dead cell stain (Thermo Fisher Scientific) to initially determine pulse parameters that induce electroporation for *P. caudatus*. The SYTOX® Blue dye cannot penetrate the plasma membrane of living cells, but easily penetrates compromised plasma membranes, such as those induced by electroporation. Thus, the only cells that fluoresce are those that are exposed to an electric field strength and duration within and above the cell-specific critical electroporation threshold. *P. caudatus* cultures at logarithmic growth phase (1×10^7 cells to 1.3×10^7) were harvested by centrifugation at 5000×*g* for 30 s. Cells were re-suspended in 200 μl of MilliQ water, 1% seawater, 10% seawater, 10% cytomix, or 50% cytomix and mixed with SYTOX® Blue dead cell stain to a final concentration of 5 μM. Cells were incubated for 2 min, then electroporated with exponential decay or microfluidic systems using different electroporation parameters. Two to three biological replicates (i.e., cells mixed with one of the tested buffer) were used for each of the tested applied voltages (technical replicates). In the exponential decay system we applied voltages of 300 V ($E_{max} = 1500$ V/cm), 500 V ($E_{max} = 2500$ V/cm), and 800 V ($E_{max} = 4000$ V/cm). For the microfluidic device we applied voltages of 500 V ($E_{max} = 3000$ V/cm) and 1000 V ($E_{max} = 6000$ V/cm) (Fig. 2). The applied voltage and pulse duration were measured for each electroporated sample and are shown in Table 1. For the exponential decay, cell integrity was confirmed using a bright field microscope (Nikon) and 20× objective (Fig. 2B–D). The bright blue signal was detected using a fluorescence microscope equipped with DAPI filter set. For the microfluidic system we were able to confirm the conditions that lead to successful entry of the SYTOX® Blue dye in real-time (Fig. 2E and F).

Plasmid selection and preparation

Three plasmids were obtained from Addgene (www.addgene.org/). pEYFP-Mitotrap (CMV mammalian and yeast promoter, the Tom70p gene targeting the outer membrane of the mitochondria in yeast and mammalian cells, and the YFP reporter) was a gift from Margaret Robinson (Addgene plasmid # 46942; Robinson *et al.*, 2010); pEF-GFP (EF1 alpha promoter from mammalian cells for expression of GFP) and pUB-GFP (mammalian Ubiquitin C promoter for expression of GFP) were gifts from Connie Cepko (Addgene plasmid # 11154 and # 11155, respectively; Matsuda and Cepko, 2004). These plasmids were used to assess the transcriptional activity of those promoters and pEYFP-Mitotrap was used to assess whether Tom70p would only be expressed within the kinetoplast (a dense DNA-containing granule within the cell's single mitochondrion). Plasmids were purified from 100 ml cultures grown overnight in standard Luria Bertani liquid medium with the appropriate selection marker. Purification was done according to the manufacturer's protocol for the Plasmid Midi Kit (Qiagen, Germantown, MD), with the following modifications: (1) Each 100 ml culture was split into two 50 ml volumes and centrifuged at 4500 rpm for 20 min at 4°C to pellet bacterial cells; (2) Each half went through the lysis steps separately, and the lysate was pooled after neutralization; (3) Pelleting of precipitated DNA was done by centrifugation at 4600 rpm for 60 min at 4°C; (4) Each 2 ml volume of pellet (in 70% ethanol wash) was split into two 1 ml volumes, centrifuged at 15 000×*g* for 10 min at 4°C, and the supernatant decanted; and (5) Dried DNA pellets were re-suspended in 50 μl of nuclease-free water, and the two 50 μl volumes were combined for each sample. Purified plasmid DNA was quantified using the Qubit fluorometer (Thermo Fisher Scientific, Waltham, MA) and stored at −20°C until use. The success of our plasmid preparations was confirmed by PCR prior to use in transfection experiments.

Transfection of P. caudatus

P. caudatus cells were grown to logarithmic phase (1×10^7 cells to 1.3×10^7) and harvested by centrifugation at 5000×*g* for 30 s, re-suspended in 200 μl cytomix (50% in distilled water), mixed with 20–40 μg of plasmid, and then transferred into an electroporation cuvette (2.0-mm gap) for electroporation with the exponential decay system and the square wave electroporation system. For the microfluidic system, cells in cytomix buffer were aspirated into 1/16 inch tygon tubing (McMaster-Carr) prior to being delivered into the microchannel. We carried out a minimum of ten trials of each combination of electroporation conditions tested using the three platforms; however, only the successful transformation parameters are summarized in Tables 1 and 2. Electroporation parameters that were not successful are included in Supporting Information Table S1 for the exponential decay system and Supporting Information Table S2 for the microfluidic system.

RT-PCR confirmation for expression of plasmids in P. caudatus

Total RNA was isolated from transformed *P. caudatus* cells using the RNEasy Mini Kit (Qiagen, Hilden, Germany). Cells were filtered onto a Durapore® PVDF 0.45 μm-pore size filter (EMD Millipore, Billerica, MA). The filter was placed in 500 μl RLT lysis buffer (RNA Isolation Kit, Qiagen, Hilden, Germany) with 143 mM β-mercaptoethanol and vortexed. Following 10 min incubation at room temperature, 350 μl of 100% ethanol were added and the lysate was purified using RNEasy Mini Kit according to the manufacturer's instructions.

Purified RNA then underwent two rounds of DNAse treatment (Jones *et al.*, 2007). First, the Turbo DNA-*free*™ Kit (Ambion®, Thermo Scientific, Waltham, MA) was used with the following modifications: (1) A total of 2 μl DNAse was added, 1 μl each time, with each addition followed by a 30 min incubation at 37°C; and (2) 0.2 μl volumes of DNAse inactivation reagent were used. Next, the RNAse-Free DNase Set was used in combination with the RNEasy Mini Kit (Qiagen, Hilden, Germany) to perform an on-column DNAse digestion, followed by column-based purification, according to the manufacturer's instructions.

First-strand cDNA synthesis and PCR amplification were performed using the One*Taq*® RT-PCR Kit (New England Biolabs, Ipswich, MA). The appropriate reverse primer (0.5 μM final conc.; see Supporting Information Table S3) and 5 μl RNA were used for reverse transcription. Control reactions were performed with water in place of the reverse transcriptase enzyme mix. cDNA was amplified in a 25 μl PCR reaction, with final primer concentrations of 0.2 μM. Thermocycling conditions were as follows: 30 s at 95°C; 30 cycles of 30 s at 94°C, 30 s at 58°C, and 30 s at 68°C; and a final extension for 5 min at 68°C. PCR primers targeting expression of the GFP or YFP reporter gene (Supporting Information Table S3) were used. PCR products were visualized by gel electrophoresis, with purified plasmid as a positive control. Amplified PCR products at the expected size of 367-bp for YFP and GFP genes were documented (Fig. 5).

Supplementary methods

Soft lithography protocol for microfluidic device fabrication

Soft lithography is employed to fabricate devices with microscale features. This process creates a master stamp from photomasks that can be used to create devices repeatedly. The photomasks are designed in AutoCAD 2014 (Autodesk, San Rafael, CA) with bilaterally converging or straight geometries, and are printed by Fine-Line Imaging (Colorado Springs, CO). The microchannels are microfabricated using soft lithography techniques described by Whitesides *et al*. (2001) and Garcia *et al*. (2016). Briefly, SU-8 (SU-8 2050, Micro-Chem, Westborough, MA) molds are patterned on silicon wafers with standard photolithography. Afterwards, the surfaces of the SU-8 master mold are treated for 2 h with tridecafluoro-1,1,2,2-tetrahydrooctyl-1-trichlorosilane (Sigma Aldrich, St. Louis, MO) under vacuum before being used for molding. Next, the SU-8 master mold polydimethylsiloxane (PDMS, Sylgard 184, Dow Corning, Midland, MI) was used at a 10:1 ratio after 2-h vacuum for removal of air bubbles in the polymer. The PDMS devices are bonded to a glass substrate after a 45 s plasma treatment and placed overnight in an oven at 75°C prior to subsequent experiments.

Acknowledgements

The authors have no conflict of interest to declare. This project was funded by the Gordon and Betty Moore Foundation through Grant GBMF4963 to V. Edgcomb, P. Girguis, and C. Buie. This work was also funded by the National Science Foundation (NSF) I-Corps 1562925 and NSF PFI:AIR - TT 1640678.

References

Azam, F., and Malfatti, F. (2007) Microbial structuring of marine ecosystems. *Nat Rev Microbiol* **5:** 782–791.

Clark, M.B., Choudhary, A., Smith, M.A., Taft, R.J., and Mattick, J.S. (2013) The dark matter rises: the expanding world of regulatory RNAs. *Essays Biochem* **54:** 1–16.

Cold, E.R., Freyria, N.J., Martinez Martinez, J., and Fernandez Robledo, J.A. (2016) An agar-based method for plating marine protozoan parasites of the genus *Perkinsus*. *PLoS One* **11:** e0155015.

Corovic, S., Pavlin, M., and Miklavcic, D. (2007) Analytical and numerical quantification and comparison of the local electric field in the tissue for different electrode configurations. *Biomed Eng Online* **6:** 37.

De Riso, V., Raniello, R., Maumus, F., Rogato, A., Bowler, C., and Falciatore, A. (2009) Gene silencing in the marine diatom *Phaeodactylum tricornutum*. *Nucleic Acids Res* **37:** e96.

Fernandez-Robledo, J.A., Lin, Z., and Vasta, G.R. (2008) Transfection of the protozoan parasite *Perkinsus marinus*. *Mol Biochem Parasitol* **157:** 44–53.

Garcia, P.A., Ge, Z., Kelley, L.E., Holcomb, S.J., and Buie, C.R. (2017) High efficiency hydrodynamic bacterial electrotransformation. *Lab Chip* **17:** 490–500.

Garcia, P.A., Ge, Z., Moran, J.L., and Buie, C.R. (2016) Microfluidic screening of electric fields for electroporation. *Sci Rep* **6:** 21238.

Gong, W., Browne, J., Hall, N., Schruth, D., Paerl, H., and Marchetti, A. (2017) Molecular insights into a dinoflagellate bloom. *ISME J* **11:** 439–452.

von der Heyden, S., Chao, E.E., Vickerman, K., and Cavalier-Smith, T. (2004) Ribosomal RNA phylogeny of bodonid and diplonemid flagellates and the evolution of euglenozoa. *J Eukaryot Microbiol* **51:** 402–416.

Hoffmeyer, T.T., and Burkhardt, P. (2016) Choanoflagellate models – *Monosiga brevicollis* and *Salpingoeca rosetta*. *Curr Opin Genet Dev* **39:** 42–47.

Hopes, A., Nekrasov, V., Kamoun, S., and Mock, T. (2016) Editing of the urease gene by CRISPR-Cas in the diatom *Thalassiosira pseudonana*. *Plant Methods* **12:** 49.

Jackson, A.P., Otto, T.D., Aslett, M., Armstrong, S.D., Bringaud, F., Schlacht, A., *et al*. (2016) Kinetoplastid phylogenomics reveals the evolutionary innovations associated with the origins of parasitism. *Curr Biol* **26:** 161–172.

Jackson, A.P., Quail, M.A., and Berriman, M. (2008) Insights into the genome sequence of a free-living Kinetoplastid: *Bodo saltans* (Kinetoplastida:Euglenozoa). *BMC Genomics* **9:** 594.

Jones, K.L., Drane, D., and Gowans, E.J. (2007) Long-term storage of DNA-free RNA for use in vaccine studies. *Biotechniques* **43:** 675–681.

Josenhans, C., Friedrich, S., and Suerbaum, S. (1998) Green fluorescent protein as a novel marker and reporter system in *Helicobacter* sp. *FEMS Microbiol Lett* **161:** 263–273.

Kaneko, T., Sakuma, T., Yamamoto, T., and Mashimo, T. (2014) Simple knockout by electroporation of engineered endonucleases into intact rat embryos. *Sci Rep* **4:** 6382.

Kim, T.K., and Eberwine, J.H. (2010) Mammalian cell transfection: the present and the future. *Anal Bioanal Chem* **397:** 3173–3178.

Knight, D.E., and Scrutton, M.C. (1986) Gaining access to the cytosol: the technique and some applications of electropermeabilization. *Biochem J* **234:** 497–506.

Kopylov, A.I., Mamaeva, T.I., and Batsanin, S.F. (1980) Energy balance of the colorless flagellate parabodo attenuatus zoomastigophora protozoa. *Okeanologiya* **20:** 1073–1078.

Kotnik, T., Frey, W., Sack, M., Haberl Meglic, S., Peterka, M., and Miklavcic, D. (2015) Electroporation-based applications in biotechnology. *Trends Biotechnol* **33:** 480–488.

Lander, N., Chiurillo, M.A., and Docampo, R. (2016a) Genome editing by CRISPR/Cas9: a game change in the genetic manipulation of protists. *J Eukaryot Microbiol* **63:** 679–690.

Lander, N., Chiurillo, M.A., Storey, M., Vercesi, A.E., and Docampo, R. (2016b) CRISPR/Cas9-mediated endogenous C-terminal tagging of *Trypanosoma cruzi* genes reveals the acidocalcisome localization of the inositol 1,4,5-trisphosphate receptor. *J Biol Chem* **291:** 25505–25515.

Lander, N., Li, Z.H., Niyogi, S., and Docampo, R. (2015) CRISPR/Cas9-induced disruption of paraflagellar rod protein 1 and 2 genes in *Trypanosoma cruzi* reveals their role in flagellar attachment. *MBio* **6:** e01012.

Liang, X., Potter, J., Kumar, S., Ravinder, N., and Chesnut, J.D. (2017) Enhanced CRISPR/Cas9-mediated precise genome editing by improved design and delivery of gRNA, Cas9 nuclease, and donor DNA. *J Biotechnol* **241:** 136–146.

Liu, X., Hempel, F., Stork, S., Bolte, K., Moog, D., Heimerl, T., *et al*. (2016) Addressing various compartments of the diatom model organism *Phaeodactylum tricornutum* via subcellular marker proteins. *Algal Res* **20:** 249–257.

Matsuda, T., and Cepko, C.L. (2004) Electroporation and RNA interference in the rodent retina *in vivo* and *in vitro*. *Proc Natl Acad Sci U S A* **101:** 16–22.

Miyahara, M., Aoi, M., Inoue-Kashino, N., Kashino, Y., and Ifuku, K. (2013) Highly efficient transformation of the diatom *Phaeodactylum tricornutum* by multi-pulse electroporation. *Biosci Biotechnol Biochem* **77:** 874–876.

Neumann, E., Schaefer-Ridder, M., Wang, Y., and Hofschneider, P.H. (1982) Gene transfer into mouse lyoma cells by electroporation in high electric fields. *J Embo* **1:** 841–845.

Opperdoes, F.R., Butenko, A., Flegontov, P., Yurchenko, V., and Lukeš, J. (2016) Comparative metabolism of free-living *Bodo saltans* and parasitic trypanosomatids. *J Eukaryot Microbiol* **63:** 657–678.

Peng, D., Kurup, S.P., Yao, P.Y., Minning, T.A., and Tarleton, R.L. (2015) CRISPR-Cas9-mediated single-gene and gene family disruption in *Trypanosoma cruzi*. *mBio* **6:** e02097–e02014.

Robinson, M.S., Sahlender, D.A., and Foster, S.D. (2010) Rapid inactivation of proteins by rapamycin-induced rerouting to mitochondria. *Dev Cell* **18:** 324–331.

Sanders, T.A., Llagostera, E., and Barna, M. (2013) Specialized filopodia direct long-range transport of SHH during vertebrate tissue patterning. *Nature* **497:** 628–632.

Teissie, J., and Tsong, T.Y. (1981) Electric-field induced transient pores in phospholipid-bilayer vesicles. *Biochemistry* **20:** 1548–1554.

Te Lohuis, M.R., and Miller, D.J. (1998) Genetic transformation of dinoflagellates (Amphidinium and Symbiodinium): expression of GUS in microalgae using heterologous promoter constructs. *Plant J* **13:** 427–435.

Tikhonenkov, D.V., Janouskovec, J., Keeling, P.J., and Mylnikov, A.P. (2016) The morphology, ultrastructure and SSU rRNA gene sequence of a new freshwater flagellate, *Neobodo borokensis* n. sp. (Kinetoplastea, Excavata). *J Eukaryot Microbiol* **63:** 220–232.

van Ooijen, G., Knox, K., Kis, K., Bouget, F.-Y., and Millar, A.J. (2012) Genomic transformation of the picoeukaryote *Ostreococcus tauri*. *J Visual Exp* **6:** e4074.

Weaver, J.C., Smith, K.C., Esser, A.T., Son, R.S., and Gowrishankar, T.R. (2012) A brief overview of electroporation pulse strength-duration space: a region where additional intracellular effects are expected. *Bioelectrochemistry* **87:** 236–243.

Whitesides, G.M., Ostuni, E., Takayama, S., Jiang, X.Y., and Ingber, D.E. (2001) Soft lithography in biology and biochemistry. *Annu Rev Biomed Eng* **3:** 335–373.

Worden, A.Z., Follows, M.J., Giovannoni, S.J., Wilken, S., Zimmerman, A.E., and Keeling, P.J. (2015) Environmental science. Rethinking the marine carbon cycle: factoring in the multifarious lifestyles of microbes. *Science* **347:** 1257594.

Supporting information

Additional Supporting Information may be found in the online version of this article at the publisher's web-site:

Fig. S1. Representative 5-ms square waveform delivered with alternating polarity in the microfluidic device at a 95% duty cycle. This device geometry results in a $\sim 6\times$ amplification of the applied voltage in the narrowest portion of the constriction. Therefore, the applied voltage of 250 V presented here results in a maximum electric field (E_{max}) of 1500 V/cm in the microfluidic device.

Fig. S2. Graphical representation of the microfluidic device used in this study for continuous flow-through transfection of *P. caudatus*. The device exhibits inlet (green) and outlet (red) fluidic ports that also serve as electrodes to generate the electric field within the bilateral constriction.

Video S1. Microfluidic electroporation of *Parabodo caudatus* in the presence of 5 μM SYTOX® Blue nucleic acid stain using an applied voltage of 1000 V ($20\times$ magnification) demonstrates successful intracellular delivery of dye due to real-time fluorescence detection.

Video S2. Microfluidic electroporation of *Parabodo caudatus* with pUB-GFP driven at 500 μl/min with an applied voltage of 375 V ($E_{max} = 2250$ V/cm) and a 50% duty cycle resulted in 20–30% transfection efficiency.

Table S1. All experimental conditions evaluated for *Parabodo caudatus* viability post-electroporation in 2-mm cuvettes using the exponential decay waveform.

Table S2. All experimental conditions evaluated for *Parabodo caudatus* transfection in the microfluidic electroporation platform in reverse chronological order. *Note: The samples treated in cytomix buffer employed a straight channel constriction in order to better compare with the square-wave pulses.

Table S3. PCR primers used in this study to verify presence of inserts in plasmids and to verify successful transfection using RT-PCR.